THE INFLUENCE OF SPECIMEN SIZE ON CREEP CRACK GROWTH RATE IN CROSS-WELD CT SPECIMENS CUT OUT FROM A WELDED COMPONENT

Peder Andersson, Peter Segle, Lars Å. Samuelson

SAQ/FoU-Report 99/04

ISSN 1401-5331

SAQ KONTROLL AB

Box 49306, SE-100 29 STOCKHOLM, Sweden

Tel: +46 8-617 40 00; Fax: +46 8-651 70 43

Preprint of paper presented at the
CAPE `99 conference, 12-16 april,
Wilderness, South Africa, 1999.

April 1999

THE INFLUENCE OF SPECIMEN SIZE ON CREEP CRACK GROWTH RATE IN CROSS-WELD CT SPECIMENS CUT OUT FROM A WELDED COMPONENT

Peder Andersson, Peter Segle and Lars Å. Samuelson
SAQ Kontroll AB, Box 49306, SE-10029 STOCKHOLM, Sweden

ABSTRACT

A 3D finite element study of creep crack growth in cross-weld CT specimens with material properties of 2.25Cr1Mo at 550 °C is carried out, where large strain and displacement theory is used. The creep crack growth rate is calculated using a creep ductility based damage model, in which the creep strain rate perpendicular to the crack plane ahead of the crack tip is integrated, considering the multiaxial stress state. The influence of specimen size on creep crack growth rate under constant load is given special attention, but the possibility to transfer results from cross-weld CT specimens to welded high temperature components is also investigated. The creep crack growth rate of a crack in a circumferentially welded pipe is compared with the creep crack growth rate of cross-weld CT specimens of three different sizes, cut out from the pipe.

Although the constraint ahead of the crack tip is higher for a larger CT specimen, the creep crack growth rate is higher for a smaller specimen than for a larger one if they are loaded to attain the same stress intensity factor. If the specimens are loaded to the same C^* value, however, a more complicated pattern occurs; depending on the material properties of the weldment constituents, the CT specimen with the intermediate size will either yield the highest or the lowest creep crack growth rate.

1. INTRODUCTION

Problems with creep cracking and creep damage in high temperature components are being given more attention as many facilities are reaching or even exceeding their design life. As a natural consequence existing assessment procedures and testing methods or standards are being reviewed. For assessments of creep cracking there are some procedures, e.g. [1], and some are under development, e.g. [2]. For creep crack growth (CCG) testing of homogeneous 'Compact Tension' (CT) specimens there is a testing standard available, i.e. ASTM E 1457 [3]. For CCG testing of cross-weld CT specimens however, a similar testing standard does not exist. Hence, there is an amount of uncertainty involved both when performing and interpreting the results of a CCG test on cross-weld CT specimens cut out from welded components.

The exact location of the crack in the weldment, the creep properties of the individual weldment constituents and the loading condition of the component, e.g. only internal pressure or a combination of internal pressure and additional axial stresses, are factors that could influence the growth rate for a creep crack in a weldment of a high temperature component. These factors have to be considered when performing a CCG test on a cross-weld CT specimen cut out from a cracked weldment in a component. Additionally, the size of the cut out CT specimen will influence the CCG rate obtained in the test.

In recently performed work on cross-weld CT specimens, the influence of starter notch location in HAZ, the differences in material properties of the weldment constituents and to

some extent the size effect have been investigated [4-6]. The results indicate that in order to make a proper CCG test on a cross-weld CT specimen cut out from a welded component, numerical simulations have to be performed in advance.

In the present study the influence of specimen size on the CCG rate in cross-weld CT specimens is investigated. Already performed studies of the growth rate of a creep crack located in a circumferential weld of a pipe is also used for comparison [7]. In these pipe weldment simulations different loading cases are tested, i.e. an axial stress or a combination of internal pressure and axial stress. Comparisons will then indicate how the growth rate of a creep crack in a circumferential weldment of a pipe is predicted by a CCG test on a cross-weld CT specimen.

2. INPUT PARAMETERS

2.1 Geometry of pipe and CT specimen

The pipe weldment and the cross-weld CT specimens consist of parent material, weld metal, and a heat affected zone, HAZ, see Fig. 1. The crack is located in the center of the HAZ and is assumed to grow within the HAZ with the crack plane parallel to the interface between the HAZ and the parent/weld metal. The CT specimens used in the finite element simulations are side grooved with a thickness reduction of 20%. The included angle of the side groove is less than 90° and the root radius is less than 0.4 mm according to the ASTM E 1457 standard [3]. Three different sizes of the CT specimens are considered, W=25 mm, W=50 mm and W=100 mm. Furthermore, the width of the HAZ is 2 mm and a/W=0.5 for all three specimen sizes. The inner and outer radius of the pipe is 200 mm and 240 mm, respectively, and the depth of the crack is 10 mm, i.e. one quarter of the wall thickness [7].

2.2 Material properties

The material properties of 2.25Cr1Mo at 550 °C are chosen for both parent and weld metal. The constitutive equation, considering elastic and creep response, is given by

$$\frac{\mathrm{d}\varepsilon_{ij}}{\mathrm{d}t} = \frac{1+\nu}{E}\left[\left(\frac{\mathrm{d}\sigma_{ij}}{\mathrm{d}t}\right) - \frac{\nu}{1+\nu}\left(\frac{\mathrm{d}\sigma_{kk}}{\mathrm{d}t}\right)\delta_{ij}\right] + \frac{3}{2}B\bar{\sigma}^{n-1}s_{ij} \qquad (1)$$

where ε_{ij}, σ_{ij} and s_{ij} are the strain, stress and stress deviator tensors respectively and $\bar{\sigma}$ is the von Mises stress. The constants in (1) are given in Table 1. Throughout the simulations, the material properties are kept constant for the weld metal and the parent material. Thus, only the material properties of HAZ is being varied.

Table 1. Material constants.

Constant	PM/WM	Creep-soft HAZ	Creep-hard HAZ
B	3.0×10^{-17}	3.0×10^{-16}	3.0×10^{-18}
n	5.7	5.7	5.7
E (MPa)	150 000	150 000	150 000
ν	0.3	0.3	0.3

2.3 Loading

In order to study the effects on creep crack growth of different overall loading conditions, the loading is varied for the pipe so that it consists of either an axial loading of 85.4 MPa or a combination of an axial loading of 85.4 MPa and an internal radial pressure of 25 MPa [7]. For both these cases the stress intensity factor for the crack becomes 20 MPa$\sqrt{\text{m}}$ [8].

For the CT specimens the loading is chosen so that the stress intensity factor K_I becomes 20 MPa$\sqrt{\text{m}}$ regardless of specimen size, where K_I is calculated according to the ASTM E 1457 standard,

$$K_I = \frac{F}{\sqrt{C\,C_N\,W^{1/2}}}\,\frac{2+a/W}{(1-a/W)^{3/2}}\,f(a/W) \qquad (2)$$

where F is the force, C (= 0.5 W) is the thickness of the specimen, C_N is the net thickness at the roots of the side grooves, W and a are defined in Fig. 1 and

$$f(a/W) = 0.886 + 4.64\,(a/W) - 13.32\,(a/W)^2 + 14.72\,(a/W)^3 - 5.6\,(a/W)^4. \qquad (3)$$

2.4 Simulated configurations

Ten different configurations are simulated for the CT specimens and four different configurations from the pipe weldment simulations in [7] will be used, see Tables 2 and 3.

Table 2. Simulated configurations of CT specimens

CT specimen Width W (mm)	B in HAZ	B in PM/WM	Remark
25	3e-16	3e-16	Homogeneous
25	3e-16	3e-17	Heterogeneous
25	3e-18	3e-17	Heterogeneous
25	3e-18	3e-18	Homogeneous
50	3e-16	3e-16	Homogeneous
50	3e-16	3e-17	Heterogeneous
50	3e-18	3e-17	Heterogeneous
50	3e-18	3e-18	Homogeneous
100	3e-16	3e-17	Heterogeneous
100	3e-18	3e-17	Heterogeneous

Table 3. Four configurations of the pipe weldment in [7].

Pipe weldment Loading combination	B in HAZ	B in PM/WM	Remark
Axial+internal pressure	3e-16	3e-17	Heterogeneous
Axial	3e-16	3e-17	Heterogeneous
Axial+internal pressure	3e-18	3e-17	Heterogeneous
Axial	3e-18	3e-17	Heterogeneous

3. FINITE ELEMENT MODELLING OF PIPES AND CT SPECIMENS

The general purpose finite element code ABAQUS [9] is used for the simulations. The 3D 20 node C3D20R element is used for the cross-weld CT specimens and in [7] the axisymmetric element CAX8R was used for the pipe weldment. The crack tip is modelled with a radius of 0.01 mm and large strain and displacement theory is utilized. The 3D simulations are due to their time consuming nature not performed until the transition time is exceeded, but until convergence in the results is obtained.

*3.1 Calculation of C**

In calculating the creep crack growth rate, the C^* integral is often used as a characterizing parameter. C* is defined through the expression

$$C^* = \int_{\Gamma}\left[W_s^* \mathrm{d}y - T_i\left(\frac{\partial \dot{u}_i}{\partial x}\right)\mathrm{d}s\right], \tag{4}$$

where W_s^* is the deformation work rate density, T_i is the outward traction vector on $\mathrm{d}s$, $\dot{u}_i$ is the displacement rate vector at $\mathrm{d}s$, x and y are coordinates in a rectangular coordinate system and finally, $\mathrm{d}s$ is the increment on the contour path Γ. This expression for C* can be calculated with for instance the finite element method.

3.2 Calculation of creep crack growth rate

The creep crack growth rate can be evaluated in a number of different ways. Usually the C^* integral is used as a measure of creep crack growth rate and for engineering applications with homogeneous materials the following approximative expression can be used [10]

$$\dot{a}\,\varepsilon_f = \frac{3\times\left(C^*\right)^{n/n+1}}{1.65\mathrm{e}^{-1.5h}}, \tag{5}$$

where n/n+1 for most engineering materials approximately is in the range between 0.7 and 1, ε_f is the uniaxial creep ductility and h is the constraint parameter defined as

$$h = \frac{\sigma_1 + \sigma_2 + \sigma_3}{3\,\overline{\sigma}} \tag{6}$$

where σ_1, σ_2, σ_3 are the principal stresses and $\overline{\sigma}$ is the von Mises stress. A finite element analysis most probably has to be performed to calculate the value of h ahead of the crack tip, since it is generally not given. Alternatively, if plane strain or plane stress prevails, the denominator in equation (5) is set to 1/50 or 1 respectively [10]. However, the approximative expression in (5) is meant for assessments of creep cracks in homogeneous materials, and it has not really been investigated whether it also applies for creep cracks in welds.

In the present study the creep crack growth rate is described by a creep ductility based damage model in which the accumulated uni-axial creep strain in a material element in front of the crack tip is considered. For the theoretical modelling, consider the crack tip with its creep process zone of accumulated creep damage as a static entity and the material in front of it as moving towards the crack tip at a constant speed $-\dot{a}$, see Fig. 2. As this material element is moving through the damaged zone, the accumulated uni-axial creep strain in the element is given by

$$\varepsilon^{c} = \int \mathrm{d}\,\varepsilon^{c} = \int_{r_c}^{r} \frac{\partial \varepsilon^{c}}{\partial t}\frac{\partial t}{\partial x}\,\mathrm{d}\,x = \int_{r_c}^{r} \dot{\varepsilon}^{c}\left(-1/\dot{a}\right)\mathrm{d}\,x = -\frac{1}{\dot{a}}\int_{r_c}^{r} \dot{\varepsilon}^{c}\,\mathrm{d}\,x. \tag{7}$$

As the element approaches the crack tip, the accumulated uni-axial creep strain in it approaches the uni-axial creep ductility, i.e. $\varepsilon^{c} \rightarrow \varepsilon_f$ as $r \rightarrow 0$. Hence,

$$\varepsilon_f = \frac{1}{\dot{a}}\int_{0}^{r_c} \dot{\varepsilon}^{c}\,\mathrm{d}\,x = \frac{1}{\dot{a}}\int_{0}^{r_c} \frac{\dot{\varepsilon}_{22}^{c}}{1.65\cdot \mathrm{e}^{-1.5h}}\,\mathrm{d}\,x, \tag{8}$$

where the last equality is due to Rice and Tracey [11]. $\dot{\varepsilon}_{22}^{c}$ is the creep strain rate perpendicular to the crack plane ahead of the crack tip, taking the multi-axial stress state into account. I.e. $\dot{\varepsilon}_{22}^{c}$ is the creep strain rate perpendicular to the crack plane calculated in the finite element simulations. Accordingly, the creep crack growth rate can be expressed as

$$\dot{a}\,\varepsilon_f = \int_{0}^{r_c} \frac{\dot{\varepsilon}_{22}^{c}}{1.65\cdot \mathrm{e}^{-1.5h}}\,\mathrm{d}\,x. \tag{9}$$

4. NUMERICAL RESULTS

Evaluations of $\dot{a}\,\varepsilon_f$ according to (9) for the ten CT specimen configurations are presented in Fig. 3. $\dot{a}\,\varepsilon_f$ is evaluated at 11 positions through the thickness of the specimens, from the center (z = 0) to the surface (z = $0.5C_N$). The results for the specimens with $B = 3\cdot 10^{-16}$ in HAZ, i.e. the creep-soft specimens, are evaluated after 30 hours and the results for the specimens with $B = 3\cdot 10^{-18}$ in HAZ, i.e. the creep-hard specimens, are evaluated after 300 hours. This difference in evaluation time is reflecting the differences in transition time between the creep-soft and creep-hard specimens, but does not exactly represent them. Since the difference in the creep strain rate between the creep-hard and the creep-soft specimens is equal to the difference in the creep constant B, given in equation (1), the same stress state occurs for the homogeneous creep-soft specimens evaluated after 30 hours as for the homogeneous creep-hard specimens evaluated after 3000 hours. However, since the calculations are very time-consuming, the simulated time had to be limited to 300 hours for the creep-hard specimens. The only effect of simulating the creep-hard specimens for longer times is that the value of $\dot{a}\,\varepsilon_f$ will attain a slightly lower value than that shown in Fig. 3.

According to Fig. 3 the creep crack growth rate is higher, for a given ductility, for smaller specimens than for larger specimens, regardless of whether the crack is located in a creep-hard

or a creep-soft HAZ, heterogeneous or homogeneous specimen. There is one exception however, when comparing the two heterogeneous CT specimens having W=100 mm and W=50 mm and $B = 3 \cdot 10^{-16}$ in HAZ, $\dot{a}\,\varepsilon_f$ is higher for the larger one. According to Fig. 3 the crack growth rate is varying along the crack front. This could be the case at the initial state of crack growth, but when steady-state conditions apply, the entire crack front will grow at the same speed. Thus, the appearance of $\dot{a}\,\varepsilon_f$ in Fig. 3 is reflecting the appearance of the crack front for the ten configurations.

The multi-axial creep strain rate perpendicular to the crack plane, $\dot{\varepsilon}_{22}^{c}$, at the center of the CT specimens (z = 0) is shown in Fig. 4. The creep strain rate is in the range of 3-10 times higher for smaller specimens than for larger, for the first 0.5 mm ahead of the crack tip. In Fig. 5 the h parameter at the center of the specimen (z = 0) is displayed for all ten CT configurations. As would have been expected, the constraint ahead of the crack tip is higher in the larger specimens than in the corresponding smaller ones.

All simulations have been performed with loadings corresponding to the same stress intensity factor, i.e. $K_I = 20\text{MPa}\sqrt{\text{m}}$. The C^* integral values corresponding to each of these configurations have been calculated as well, and in Fig. 6 $\dot{a}\,\varepsilon_f$ is displayed versus C^* for the ten CT specimens and the four pipe weldment configurations of [7]. A straight line has been drawn through each of the data points corresponding to the homogeneous CT specimens. The slope of each of these straight lines is given by the exponent n/n+1 of equation (5).

Fig. 6 reveals a number of interesting details. If the two creep-hard homogeneous CT specimens (W=25 and 50 mm with $B = 3 \cdot 10^{-18}$ in HAZ, PM and WM) were loaded to the same C^* value, the larger CT specimen would predict a higher value of $\dot{a}\,\varepsilon_f$. Similarly, if the two creep-soft homogeneous CT specimens (W=25 and 50 mm with $B = 3 \cdot 10^{-16}$ in HAZ, PM and WM) were loaded to the same C^* value, the larger specimen would predict a higher $\dot{a}\,\varepsilon_f$.

However, when it comes to comparing the heterogeneous CT specimens, difficulties arise. If the homogeneous CT specimen with W=25 mm and $B = 3 \cdot 10^{-18}$ would be loaded to the same C^* value as the heterogeneous CT specimen with W=25 mm and $B = 3 \cdot 10^{-18}$ in HAZ, the creep crack growth rate times ductility would be higher in the homogeneous specimen than in the heterogeneous one. The opposite prevails for the CT specimens with W=50 mm and $B = 3 \cdot 10^{-18}$. On the other hand, if the homogeneous CT specimen with W=25 mm and $B = 3 \cdot 10^{-16}$ would be loaded to the same C^* value as the heterogeneous CT specimen with W=25 mm and $B = 3 \cdot 10^{-16}$ in HAZ, the creep crack growth rate times ductility would be lower in the homogeneous specimen than in the heterogeneous one. The opposite prevails for the CT specimens with W=50 mm and $B = 3 \cdot 10^{-16}$. If heterogeneous CT specimens with $B = 3 \cdot 10^{-18}$ in HAZ and W=25 mm, 50 mm and 100 mm would be loaded to the same C^* value, it is according to Fig. 6 likely that the smallest specimen would yield the lowest creep crack growth rate and the specimen with W=50 mm would yield the highest rate, while the largest specimen would yield an intermediate creep crack growth rate. If heterogeneous CT specimens with $B = 3 \cdot 10^{-16}$ in HAZ and W=25 mm, 50 mm and 100 mm would be loaded to the same C^* value, the creep crack growth rates obtained would according to Fig. 6

be highest for the largest specimen, lowest for the specimen with W=50 mm and an intermediate creep crack growth rate would be obtained for the smallest CT specimen.

Although the dependence between $\dot{a}\,\varepsilon_f$ and C^* is not known for the pipe weldment, it is likely that their relation could be described with a similar expression as (5) and that the exponent is nearly n/n+1. Thus, the dependence between $\dot{a}\,\varepsilon_f$ and C^* for the pipe weldment could probably be described by a straight line nearly parallel with the lines in the diagram describing the dependence between $\dot{a}\,\varepsilon_f$ and C^* for the homogeneous CT specimens. Thus, changing the loading condition, from axial loading to a combination of axial loading and internal pressure, under constant C^*, would probably only lead to a minor change in $\dot{a}\,\varepsilon_f$ for the crack in the pipe weldment.

5. DISCUSSION AND CONCLUSIONS

When comparing different CT specimens loaded to the same stress intensity factor K_I, the creep crack growth rate is predicted to be higher for (most) smaller CT specimens than for larger ones, despite the fact that the constraint ahead of the crack tip is higher in the larger specimens. The explanation is that the creep strain rate perpendicular to the crack plane is so much higher for the smaller CT specimens than for the larger CT specimens, i.e. the differences in strain rate dominates over the differences in constraint.

When, instead, comparing the CT specimens loaded to the same C^* value, another situation arises. For the homogeneous CT specimens, a higher creep crack growth rate is predicted for the larger specimen than for the smaller specimen. For the heterogeneous CT specimen with $B = 3 \cdot 10^{-16}$ in HAZ the highest creep crack growth rate is obtained with the largest specimen, while for the heterogeneous CT specimen with $B = 3 \cdot 10^{-18}$ in HAZ the specimen with the intermediate size yields the highest creep crack growth rate.

The pipe weldment simulations reveal that changing the overall loading conditions from axial loading to a combination of axial loading and internal pressure under constant C^*, probably does not affect the creep crack growth rate significantly.

In order to transfer results from testing of a CT specimen to the component from which it was cut out, an individual matching of loading has to be done. Fig. 6 shows that a CT specimen with W=100 mm should be cut out from the pipe with $B = 3 \cdot 10^{-16}$ in HAZ; regardless whether the pipe weldment is loaded axially only or by a combination of an axial loading and an internal radial pressure, the CT specimen with W=100 mm will yield approximately the same $\dot{a}\,\varepsilon_f$ for a given C^* value as both pipe weldment configurations. For the pipe weldment with $B = 3 \cdot 10^{-18}$ in HAZ, a cut out CT specimen with W=100 mm will yield a slightly lower value of the creep crack growth rate than the pipe weldment configurations, whereas a cut out CT specimen with W=50 mm will yield a slightly higher value.

The results of the present study indicate that before an experiment is being made, it could be helpful to perform a numerical study, e.g. in order to decide the size of the CT specimen to be cut out and to select the proper loading. This could enhance the possibilities to transfer results

from the cut out specimen to the component and improve the quality of laboratory CCG testing. The purpose of performing a creep crack growth experiment must be to as best as possible imitate the near crack environment in the real component. Since the creep crack growth rate is given by equation (9), this expression could be evaluated, as described in the present study, both for a CT specimen and for the component in order to find the proper loading for the experiment.

ACKNOWLEDGEMENTS

The financial support of SAQ Kontroll AB is greatly appreciated.

REFERENCES

[1] Ainsworth, R.A., editor. R5: An assessment procedure for the high temperature response of structures, Nuclear Electric procedure R5 Issue 2 (1996).

[2] Validation, Expansion and Standardisation of Procedures for High Temperature Defect Assessment (HIDA), Project Programme of Brite/EuRam, Project BE 1702 (1995).

[3] Standard test method for measurement of creep crack growth rates in metals, ASTM E-1457-92 (1992).

[4] Segle, P., Andersson, P. and Samuelson, L.Å. (1998) A parametric study of creep crack growth in heterogeneous CT specimens by use of finite element simulations, Proceedings of the International 'HIDA' Conference, April 15-17, Paris, France.

[5] Segle, P., Andersson, P. and Samuelson, L.Å. (1998) Numerical investigation of creep crack growth in cross-weld CT specimens - Part I: Influence of mis-match in creep properties and notch tip location, submitted for publication and presented at the International Conference on 'Integrity of high-temperature welds', November 3-4, Nottingham, UK.

[6] Andersson, P., Segle, P. and Samuelson, L.Å. (1998) Numerical investigation of creep crack growth in cross-weld CT specimens - Part II: Influence of specimen size, submitted for publication and presented at the International Conference on 'Integrity of high-temperature welds', November 3-4, Nottingham, UK.

[7] Samuelson, L. Å., Andersson, P. and Segle, P. (1999) Finite element simulations of creep crack growth in welded pipes and CT specimens, To be presented at the 1999 ASME PVP Conference in Boston, USA.

[8] Andersson, P., Bergman, M., Brickstad, B., Dahlberg, L., Nilsson, F. and Sattari-Far, I.: A procedure for safety assessment of components with cracks - handbook. 3rd revised edition. SAQ/FoU-Report 96/08, SAQ Kontroll AB, Stockholm, Sweden, 1996.

[9] ABAQUS (1996) User's manual, Version 5.6, Hibbit, Karlsson and Sorenson Inc.

[10] Webster, G.A. and Ainsworth, R.A. (1994) High Temperature Component Life Assessment, Chapman & Hall, London, UK.

[11] Rice, J.R. and Tracey, D.M. (1969) On the ductile enlargement of voids in triaxial stress fields, J. Mech. Phys. Solids, Vol. 17, pp. 102-217.

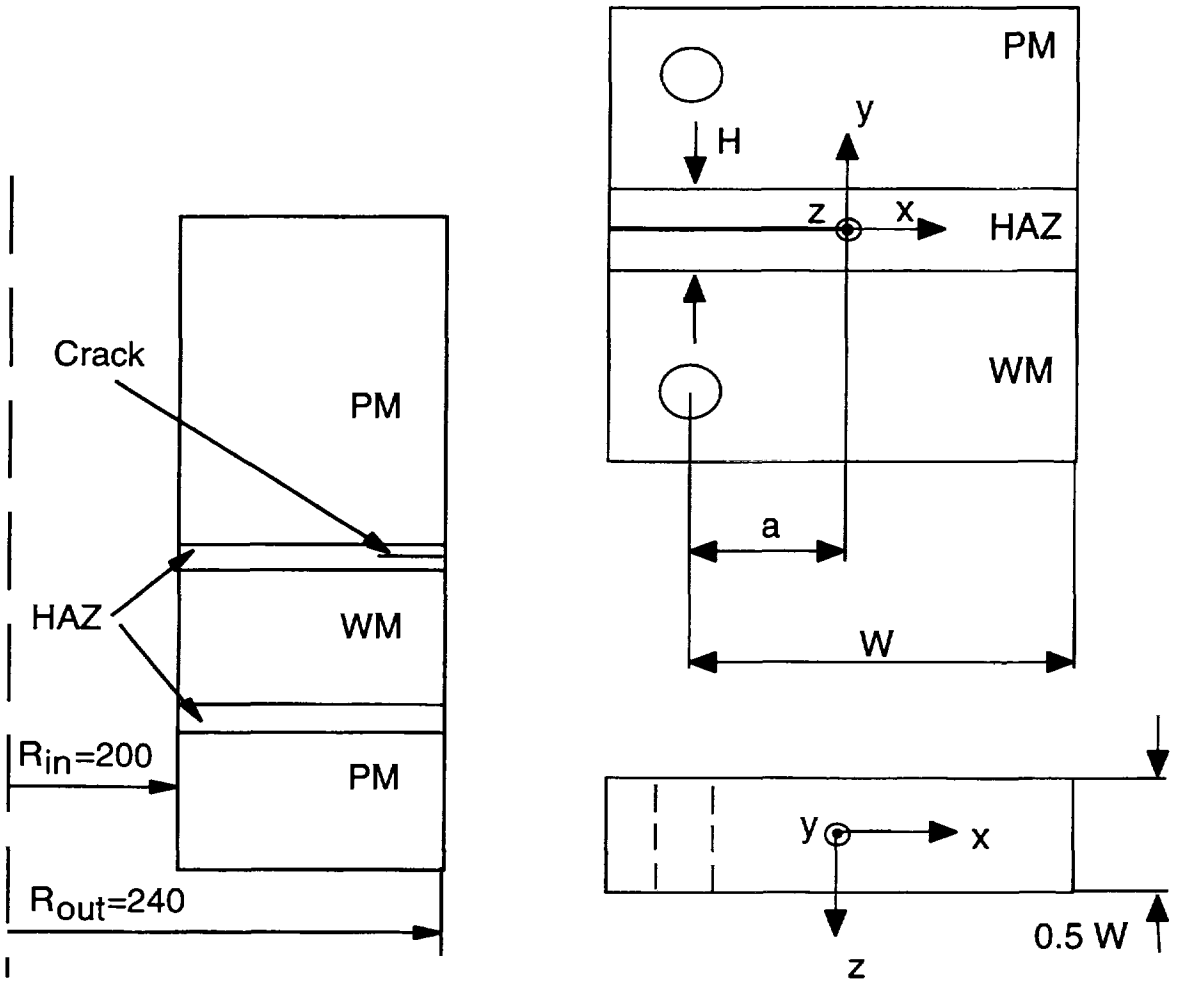

Fig. 1. a) Pipe weldment with a circumferential crack located in the HAZ [7]. b) Cross-weld CT specimen showing weldment constituents and the starter notch position. The specimens used in the finite element simulations are side grooved with a total thickness reduction of 20%. The included angle of the side groove is less than 90° and the root radius is less than 0.4 mm according to the ASTM E 1457 standard.

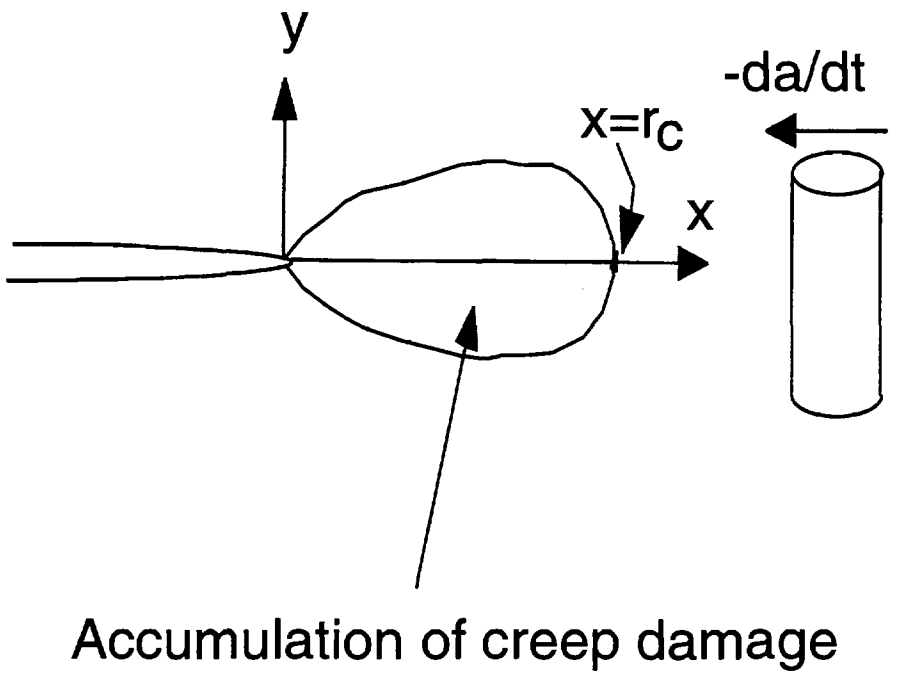

Fig. 2. The creep crack growth rate is described by a creep ductility based damage model. Creep damage is accumulated in a material element as it moves towards the crack tip.

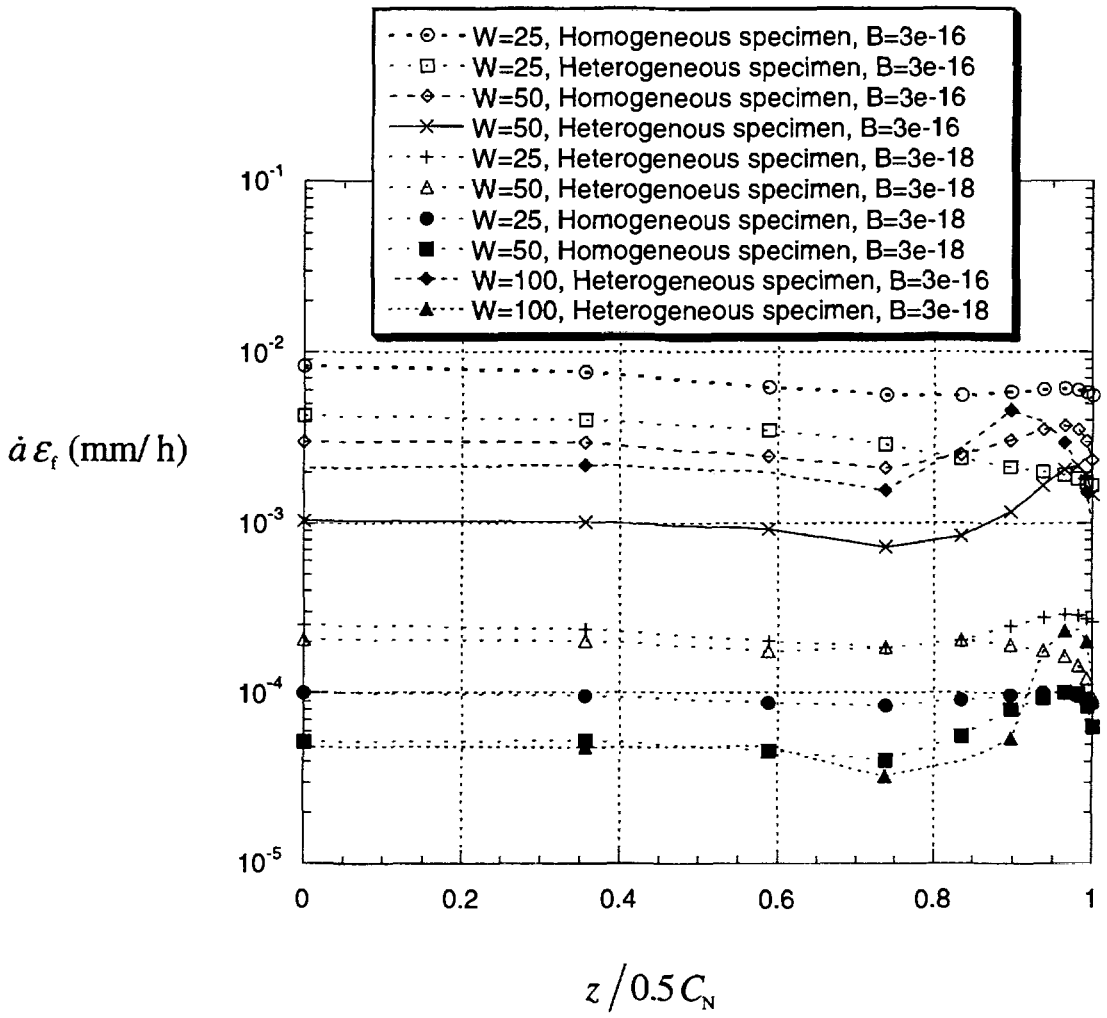

Fig. 3. The creep crack growth rate times the uni-axial creep ductility evaluated at 11 positions through the thickness of the specimens for all ten CT specimen configurations.

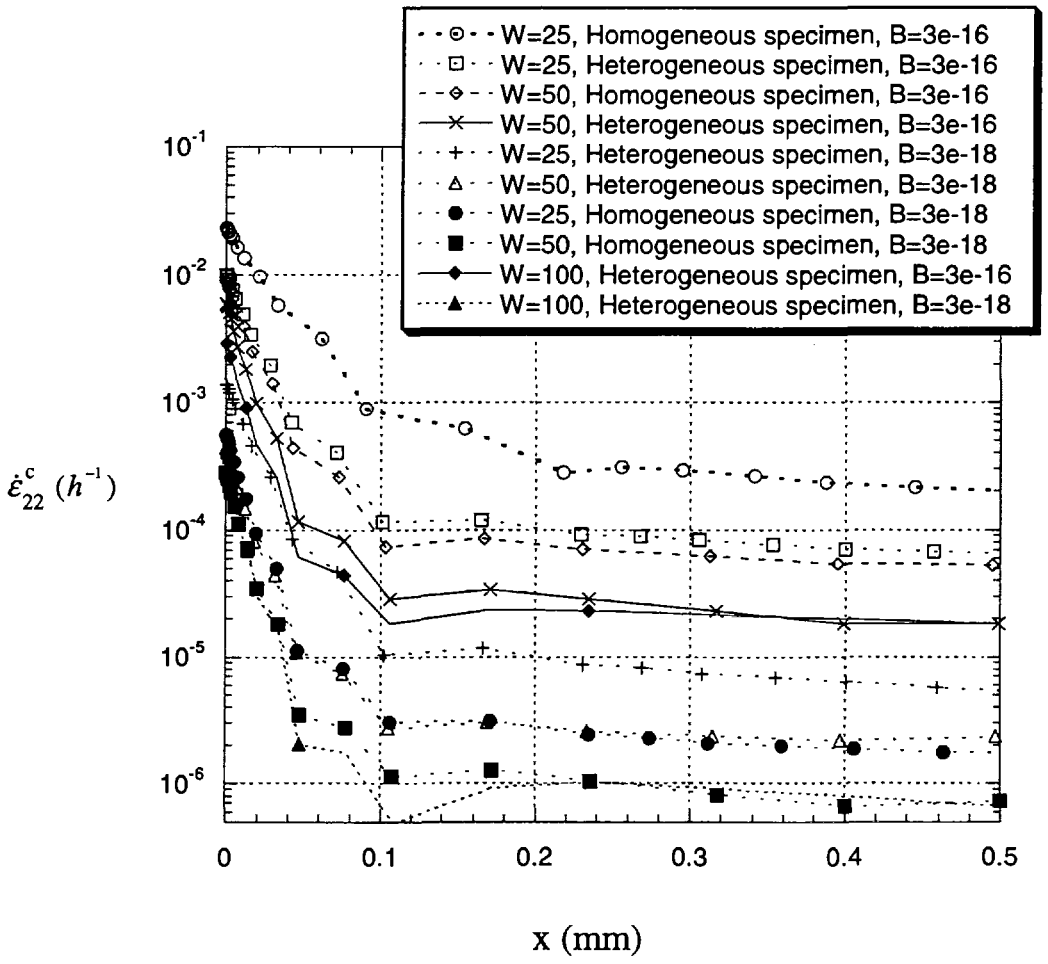

Fig. 4. The creep strain rate perpendicular to the crack plane, ahead of the crack tip, in the center of the specimens (z = 0) for all ten CT specimen configurations.

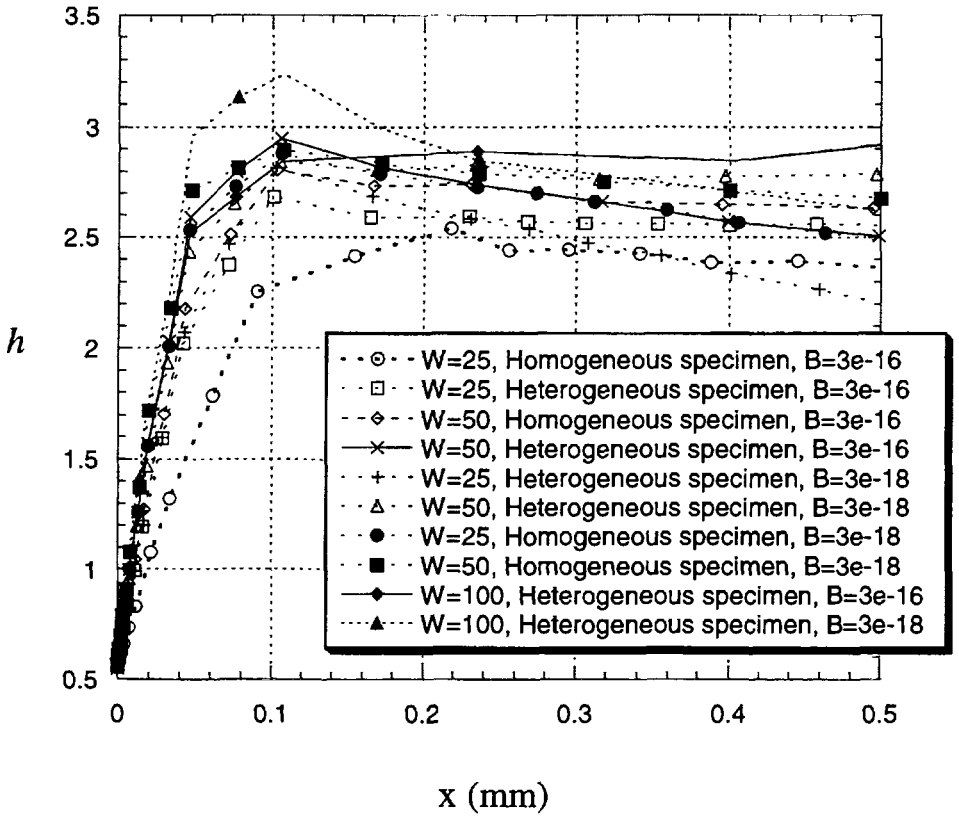

Fig. 5. The h parameter, ahead of the crack tip, in the center of the specimens ($z = 0$) for all ten CT specimen configurations.

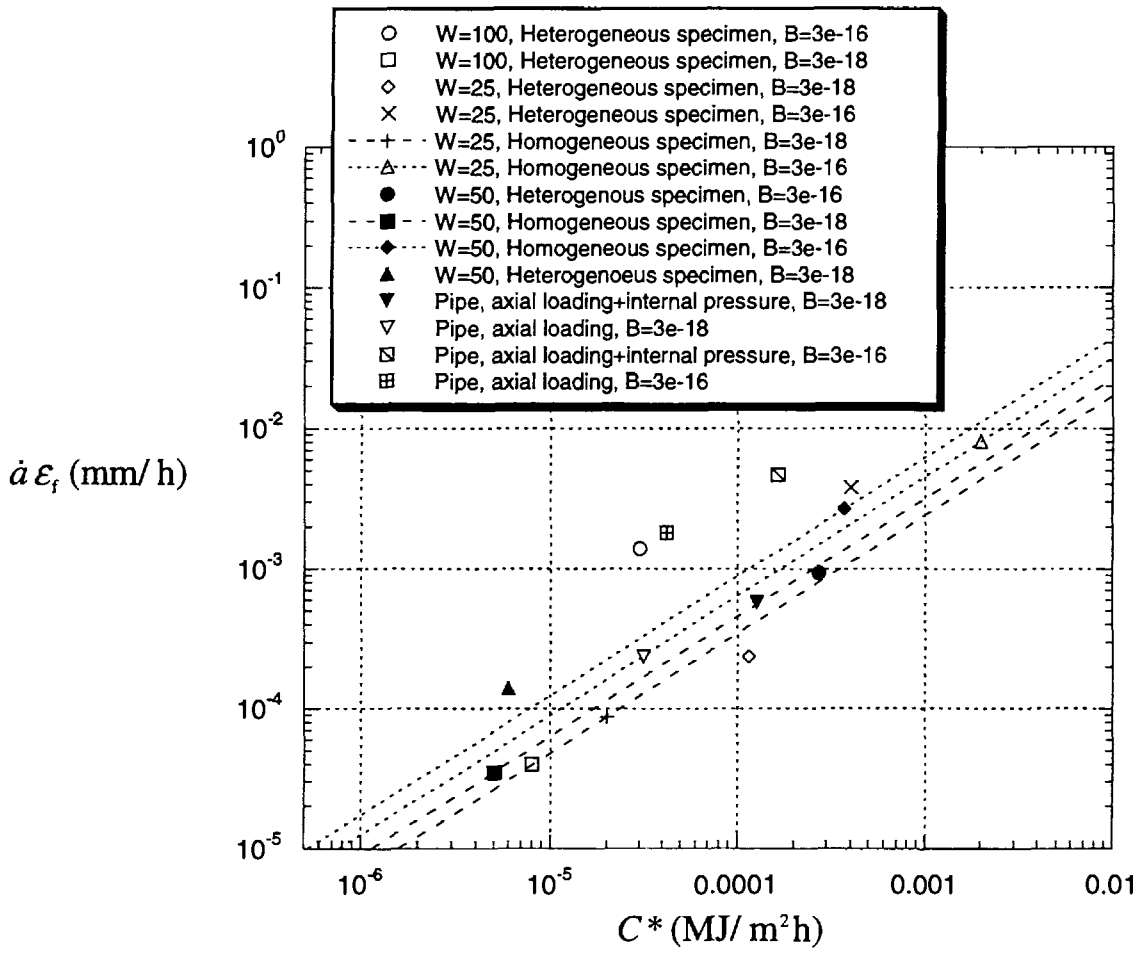

Fig. 6. The creep crack growth rate times the uni-axial creep ductility versus C^* evaluated at the center of the specimens for all ten CT specimen configurations and for the four pipe configurations.